

Electronic structure and localized states in a model amorphous silicon

G. Allan, C. Delerue, and M. Lannoo

Institut d'Electronique et de Microélectronique du Nord, Département Institut Supérieur d'Electronique du Nord, Boîte Postale 69, 59652 Villeneuve d'Ascq Cedex, France

(Received 23 October 1997)

The electronic structure of a model amorphous silicon (a -Si) represented by a supercell of 4096 silicon atoms [B.R. Djordjevic, M.F. Thorpe, and F. Wooten, Phys. Rev. B **52**, 5685 (1995)] and of a model hydrogenated amorphous silicon (a -Si:H) that we have built from the a -Si model are calculated in the tight-binding approximation. The band edges near the gap are characterized by exponential tails of localized states induced mainly by the variations in bond angles. The spatial localization of the states is compared between a -Si and a -Si:H. Comparison with experiments suggests that the structural models give good descriptions of the amorphous materials. [S0163-1829(98)00512-8]

I. INTRODUCTION

The determination of the electronic structure of materials remains of great importance since it gives access to electrical and optical properties. In crystalline materials, this is quite simplified as the crystal atomic structure is easily determined by experiment. This is no more the case for amorphous materials as one only measures average quantities like structure factors or pair distribution functions. From the theoretical point of view, the amorphous atomic structure can be obtained by total-energy minimization but for first-principles models of the electronic structure, such a procedure remains limited to periodic clusters containing about a hundred atoms.

Recently, large (4096-atom supercell) computer-generated continuous network models of tetrahedrally bonded amorphous carbon and silicon have been constructed such as the Wooten-Winer-Weaire (WWW) model.^{1,2} This one reproduces with good accuracy the experimental radial distribution function of amorphous silicon (a -Si) and for a smaller unit cell (216-atom model) calculations of the first-order Raman spectrum are in very good agreement with the experimental one,³ which, as a test to measure the credibility of structural models,⁴ gives confidence that the WWW a -Si model is a realistic one. We have calculated its electronic structure in the tight-binding approximation. This exhibits a large number of deep and strongly localized states that correspond to the well-known band tails in the amorphous semiconductor band gap. Such a large band tailing is attributed to a small number of bond angles that deviate greatly from the tetrahedral 109° value.

The paper is divided as follows. In Sec. II, we describe the a -Si:H supercell created by hydrogenation of the a -Si atomic model. In Sec. III, we present the numerical techniques that allow us to treat very large supercells. We calculate the density of states before and after "hydrogenation" to verify that the deeper states in the band gap of a -Si:H have disappeared. We show that exponential band tails occur at the gap edges. The band-tail slopes are compared to experiment for both the a -Si and a -Si:H models. The band offsets between crystalline and amorphous silicon are also deter-

mined. In the last section, the localization of the states close to the gap is calculated.

II. a -Si:H MODEL

In this section, we describe the procedure used to build the a -Si:H model starting from the original WWW model. The Si atoms that give rise to the a -Si localized states are first determined. For this, we "cut" small clusters (with about 50 Si atoms) centered on every atom of the supercell and saturate the dangling bonds of each cluster with hydrogen atoms. Then the highest occupied molecular orbital (HOMO) and the lowest unoccupied one (LUMO) are calculated in the tight-binding approximation as described in the next section. When we look at the clusters with the smallest gaps, the corresponding HOMO and LUMO states are found mainly localized on the same atom with strong bond distortions. These central atoms are removed one by one and the four dangling bonds created by the atom removal are saturated with hydrogen atoms as in Ref. 5. This is a somewhat empirical procedure but a first-principles total-energy calculation of hydrogen atom positions is not feasible for such a large supercell. Such a procedure also gives rise to the largest elastic relaxation energy gain one can expect and at the end it must produce a situation close to an optimized a -Si:H structure. Let us notice that even if the atoms are in equilibrium positions and the atomic forces are equal to zero, the supercell remains under strain. This can easily be seen when one cuts a cluster or a slab in the supercell, the slab or cluster atoms must again be relaxed. The final concentration of hydrogen atoms is equal to 8% (83 silicon atoms were removed). Once this is done the atomic positions and the supercell lattice parameter are again relaxed by use of a Keating potential⁶ as in the original WWW model. This also reduces the density of our a -Si:H model. The optimal density of the a -Si WWW model is 3% larger than the crystalline one but is difficult to compare with experimental results as it does not seem to be accurately known. However, recent measurements have found a -Si 1.8% less dense than crystalline silicon (c -Si).⁷ Let us also recall that the original WWW model does not include voids.

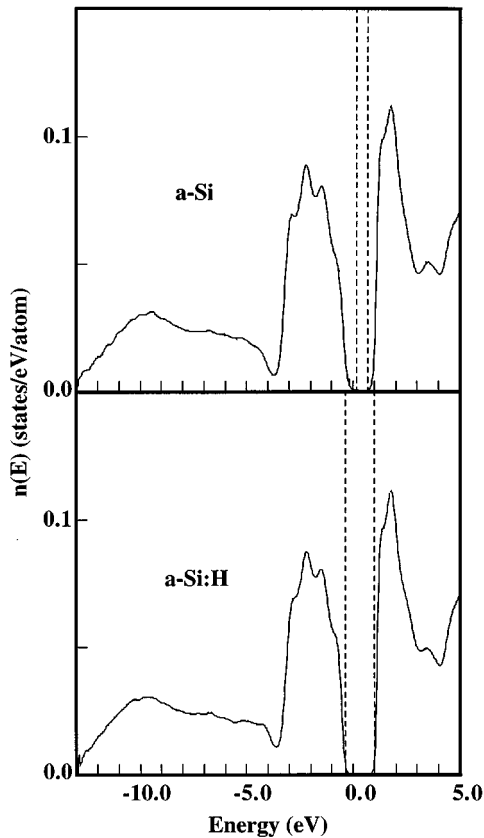


FIG. 1. Average density of states of *a*-Si (a) and *a*-Si:H (b) as calculated by the recursion method. The dotted lines indicate the limits of the gap.

III. *a*-Si AND *a*-Si:H DENSITY OF STATES

The electronic structure of the *a*-Si and *a*-Si:H supercells has been calculated in the tight-binding sp^3s^* Vogl's approximation.⁸ Even if it is a first-nearest-neighbor model, the bulk *c*-Si band gap that is fitted is in good agreement with the experimental values. The model cannot be used to accurately determine states high in the conduction band as the resulting *c*-Si conduction bands are rather flat.⁹ This is not too important in this calculation as the conduction-band edge will always remain close to bulk *c*-Si one. We take a usual d^{-2} variation of the tight-binding parameters with the interatomic distance d .¹⁰ Harrison's parameters¹⁰ are used for the first-nearest-neighbor Si-H interaction parameters. Only the Γ point at the center of the supercell cubic Brillouin zone has been used since, due to the large size of the supercell, we expect a negligible dispersion of the energies versus wave vector. The local densities of states on each atom of the supercell are approximated by a continued fraction the 40 first coefficients of which are calculated by the recursion method.¹¹ A semielliptic termination is used and their values are determined by a linear prediction method.¹² Such a procedure uses 80 exact moments of the density of states, which is sufficient to get converged results.¹³

Figure 1 shows the average density, which is close to those obtained in preceding calculations.¹⁴ The amorphous silicon valence-band width is slightly larger than the *c*-Si one. This seems to be due to the variation of the interatomic distances in the amorphous phase as the shift of the bottom

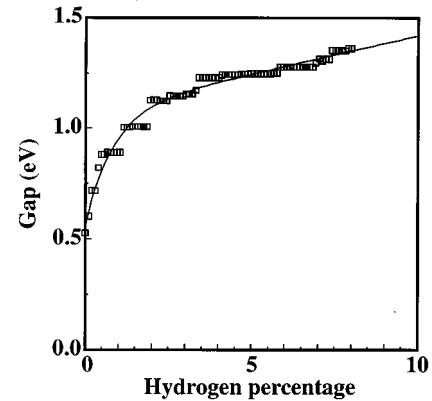


FIG. 2. Variation of the supercell gap as a function of hydrogen percentage H%. The silicon atoms are removed one by one from the *a*-Si supercell (square dots). The full line is a least-square fit giving the gap (in eV) equal to $1.074 + 0.034 \cdot H\% - 0.513 \cdot \exp(-1.202 \cdot H\%)$.

of the band (~ 0.3 eV) disappears when the variation of the interatomic tight-binding parameters with the distance is suppressed. The main difference between *a*-Si and *a*-Si:H occurs near the band gap. We see that the "hydrogenation" has suppressed the deep states in the gap. To get more precise information about these states, one has to diagonalize the Hamiltonian H . For this, we have used a Fletcher-Reeves nonlinear conjugate-gradient minimization¹⁵ of the Rayleigh quotient $\langle \Psi | (H - \sigma I)^2 | \Psi \rangle / \langle \Psi | \Psi \rangle$ with respect to the trial function Ψ . σ is an energy shift close to the band gap. This method is similar to the one used for large clusters with the empirical pseudopotential method.¹⁶ Due to the sparseness of the tight-binding Hamiltonian matrix, this method is very fast to determine the gap-edge states. Orthogonalization of the trial function to the already determined eigenstates can be used to get other states in the valence or conduction bands.

As the supercell is finite, the limits of the band gap are well defined and are equal to $(-0.36, 1.00$ eV) for *a*-Si:H and $(0.19, 0.72$ eV) for *a*-Si. We shall see below that the *a*-Si band edges correspond to states strongly localized on a few atoms whereas in the *a*-Si:H case, they correspond to moderately localized states. One must notice that these values do not depend very much on the variation of the interatomic distances. For example, the top of the *a*-Si:H valence band is simply shifted by 0.04 eV when the variation of the tight-binding parameters with interatomic distance is neglected and when all are taken equal to the *c*-Si ones. This shows that the variation of the band-gap limits is mainly due in the amorphous phases to bond angle distortions. Figure 2 shows the variation of the band gap as a function of the hydrogen percentage. A least-square fit gives a variation of 34 meV per hydrogen percent. This is larger than the value measured for the optical band gap (12.7 meV per hydrogen percent¹⁷). This may be due to the fact that as we shall see below, we are still hydrogenating moderately localized states and the gap variation is larger than for a more delocalized state.

The band lineups between crystalline and amorphous silicon can be obtained from these gap values if one knows the electrostatic dipole layer at a heterojunction between these

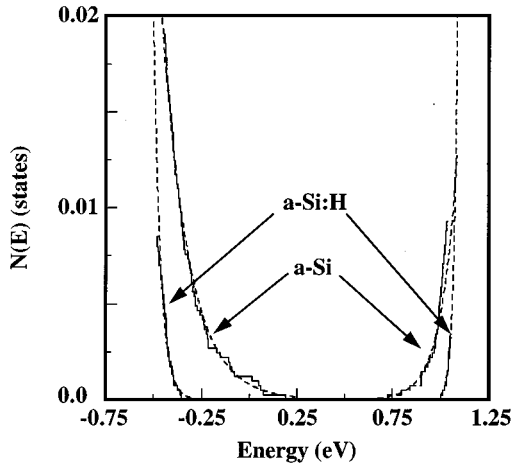


FIG. 3. Integrated density of states near the band gap (full line). The exponential fit (dotted line) is almost indistinguishable from the staircase integrated density. The two inner curves correspond to *a*-Si and the outer ones to *a*-Si:H.

materials. In the molecular model and in the zero charge-transfer approximation, which has been often used for semiconductor heterojunctions,¹⁸ the electrostatic dipole layer is just equal to the opposite of the energy difference between the hybrid orbitals on silicon atoms close to the heterojunction. The average bond angle for the *a*-Si:H model, which is equal to 109.27° is very close to the *c*-Si one, which is de-

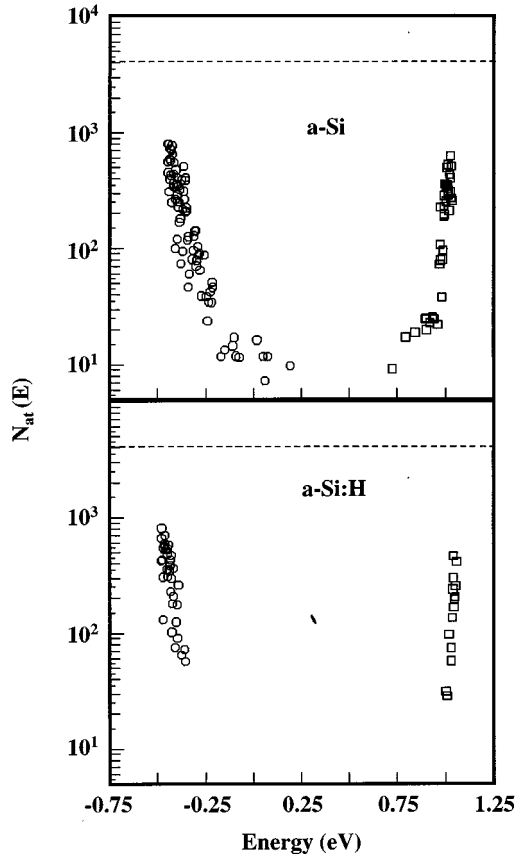


FIG. 4. Spatial localization of the band tail states. The dotted line indicates the number of Si atoms in the supercell.

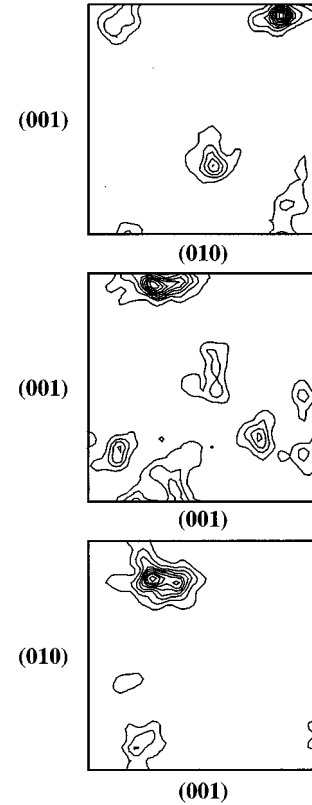


FIG. 5. Isovalues of the electronic density for a valence state localized 0.13 eV below the gap edge. The curves are shown in three orthogonal planes passing through the maximum density point.

termined by the 109.47° tetrahedral bond angle so that the mean hybrid orbital energy in *a*-Si will be close to the *c*-Si. Using c_s and c_p the average *s* and *p* characters for the valence band that one can calculate using the recursion method ($c_s + c_p = 4$), one can define an average hybrid orbital $(c_s E_s + c_p E_p)/4$ for *c*-Si, *a*-Si, and *a*-Si:H where E_s and E_p are the *s* and *p* Si orbital energies, respectively. The energy difference between the amorphous and crystalline silicon is less than 0.02 eV. So the electrostatic dipole layer at the heterojunction between these materials is negligible. The valence-band offset is thus directly obtained from the limits of the band gap discussed before. It is then equal to 0.36 eV between *a*-Si:H and *c*-Si (with a valence band higher in *c*-Si) and equal to -0.19 eV between *a*-Si and *c*-Si (with a valence band higher in *a*-Si) in agreement with recent *ab initio* pseudopotential calculation for a smaller supercell.¹⁹ For *a*-Si:H, this is also in agreement with the experimental results, which vary from 0 to 0.71 eV (Ref. 19) depending on preparation conditions of the amorphous materials.

The density of states due to localized states in amorphous semiconductors is often assumed to decay exponentially away from the conduction and valence-band edges.²⁰⁻²² This would also be true for the integrated density. Figure 3 shows the fit of the staircase integrated density by exponential curves $\exp(-|E|/E_0)$, where E_0 is the band tail slope. Figure 2 also shows that at least in this energy range, the band tails decay exponentially with slopes E_0 equal to 142 meV and 81 meV respectively for the *a*-Si valence and conduction bands.

These values are reduced to 37 meV and 19 meV for *a*-Si:H. The values for *a*-Si:H are slightly smaller than the experimental ones which are in the range of 43–103 meV (for the valence-band tail) and 27–37 meV (for the conduction one).^{20–24} Let us recall that due to the finite size of the supercell, we do not have very large wavelength lattice distortions. Their effect will be to spread the band tails we have obtained and then to slightly increase the slope values we have calculated.

IV. *a*-Si AND *a*-Si:H STATES LOCALIZATION

The spatial localization of the states is another interesting property of the band tails. We shall characterize this localization by

$$N_{\text{at}}(E_j) = \left(\sum_i \left(\sum_{l=1}^5 a_{il}^2 \right)^2 \right)^{-1}, \quad (1)$$

where the sum is extended to all the supercell atoms \mathbf{R}_i and to the $5 sp^3 s^*$ atomic functions $\phi_l(\mathbf{r} - \mathbf{R}_i)$, the tight-binding eigenfunction for the energy E_j being equal to

$$\psi_j = \sum_{i,l} a_{il} \phi_l(\mathbf{r} - \mathbf{R}_i). \quad (2)$$

When an eigenstate is completely uniform over n atoms, we have $\sum_{l=1}^5 a_{il}^2 = 1/n$ and $N_{\text{at}}(E_j)$ is just equal to n . So $N_{\text{at}}(E_j)$ gives an order of magnitude of the number of atoms on which the state is localized. Figures 4 shows this localization for the states close to the gap. For *a*-Si, states close to the band edges are found to be localized on about 10 atoms. Such states are suppressed by the hydrogenation. Neverthe-

less for *a*-Si:H, the gap edges are still localized on a few tens of atoms. This number rapidly increases as one goes deeper, for example, in the valence band but 0.15 eV below the valence-band edge, the states still extend over less than a thousand atoms. Figure 5 shows isovalues of the electronic density obtained when one broadens one eigenstate local atomic occupations $\sum_{l=1}^5 a_{il}^2$ by Gaussians centered on each lattice site. The extension of such a state 0.13 eV below the valence-band edge given by $N_{\text{at}}(E_j)$ is close to 808 atoms. This number is sufficiently small for us to think that we have not yet reached the mobility gap.

V. CONCLUSION

We have shown that large supercell models of *a*-Si (Ref. 2) and *a*-Si:H give rise to exponential band tails of localized states in the band gap. The degree of localization of the states strongly depends on their energy in the gap and on the hydrogenation of the material. The analysis of the density of states, of the slope of the tails, of the band offsets with crystalline silicon and of the localization factors suggest that these structural models are good representations of the materials.

ACKNOWLEDGMENTS

We would like to thank Dr. B. R. Djordjevic, Dr. M. F. Thorpe, Dr. F. Wooten, and Dr. D. Weaire for providing the coordinates and neighbor tables of the silicon amorphous network we have used. The “Institut d’Electronique et de Microélectronique du Nord” is “Unité Mixte 9929 du Centre National de la Recherche Scientifique.”

¹F. Wooten, K. Winer, and D. Weaire, Phys. Rev. Lett. **54**, 1392 (1985); F. Wooten and D. Weaire, Solid State Phys. **40**, 1 (1987).

²B. R. Djordjevic, M. F. Thorpe, and F. Wooten, Phys. Rev. B **52**, 5685 (1995).

³M. Marinov and N. Zotov, Phys. Rev. B **55**, 2938 (1996).

⁴N. Maley, D. Beeman, and J. S. Lannin, Phys. Rev. B **38**, 10 611 (1988).

⁵P. A. Fedders and D. A. Drabold, Phys. Rev. B **47**, 13 277 (1993).

⁶P. N. Keating, Phys. Rev. **145**, 637 (1966).

⁷J. S. Custer, M. A. Thompson, D. C. Jacobson, J. M. Poate, S. Roorda, W. C. Sinke, and F. Spaepen, Appl. Phys. Lett. **64**, 437 (1994).

⁸P. Vogl, H. P. Hjalmarson, and J. D. Dow, J. Phys. Chem. Solids **44**, 365 (1983).

⁹C. Delerue, M. Lannoo, and G. Allan, Phys. Rev. Lett. **76**, 3038 (1996).

¹⁰W. A. Harrison, *Electronic Structure and the Properties of Solids* (Freeman, San Francisco, 1980).

¹¹R. Haydock, *Solid State Physics* (Academic Press, New York, 1980), Vol. 35, p. 216.

¹²G. Allan, J. Phys. C **17**, 3945 (1984).

¹³J. Dong and D. A. Drabold, Phys. Rev. B **54**, 10 284 (1996).

¹⁴J. M. Holender and G. J. Morgan, J. Phys. C **4**, 4473 (1992).

¹⁵W. H. Press, S. A. Teukolsky, W. T. Vetterling, and B. P. Flannery, *Numerical Recipes in Fortran* (Cambridge University Press, Cambridge, 1992).

¹⁶L. W. Wang and A. Zunger, J. Phys. Chem. **98**, 2158 (1994).

¹⁷G. Kaniadakis, *Properties of Amorphous Silicon* (INSPEC, London, 1989), p. 269.

¹⁸C. Priester, G. Allan, and M. Lannoo, J. Vac. Sci. Technol. B **6**, 1290 (1988).

¹⁹C. G. Van de Walle and L. H. Yang, J. Vac. Sci. Technol. B **13**, 1635 (1995).

²⁰T. Tiedje, J. M. Cebulka, D. L. Morel, and B. Abele, Phys. Rev. Lett. **46**, 1425 (1981).

²¹K. Winer, I. Hirabayashi, and L. Ley, Phys. Rev. Lett. **60**, 2697 (1988).

²²S. Aljishi, J. D. Cohen, S. Jin, and L. Ley, Phys. Rev. Lett. **64**, 2811 (1990).

²³C.-Y. Huang, S. Guha, and S. J. Hudgens, Phys. Rev. B **27**, 7460 (1983).

²⁴T. Muschik, R. Schwarts, and F. Karg, J. Lumin. **48-9**, 636 (1991).